J. Fluid Mech. (2011), *vol.* 680, *pp.* 321–335. © Cambridge University Press 2011
doi:10.1017/jfm.2011.165

Exact tensor closures for the three-dimensional Jeffery's equation

STEPHEN MONTGOMERY-SMITH[1], WEI HE[1], DAVID A. JACK[2]† AND DOUGLAS E. SMITH[3]

[1]Department of Mathematics, University of Missouri, Columbia, MO 65211, USA

[2]Department of Mechanical Engineering, Baylor University, Waco, TX 76798, USA

[3]Department of Mechanical and Aerospace Engineering, University of Missouri, Columbia, MO 65211, USA

(Received 25 June 2010; revised 19 January 2011; accepted 1 April 2011; first published online 24 May 2011)

This paper presents an exact formula for calculating the fourth-moment tensor from the second-moment tensor for the three-dimensional Jeffery's equation. Although this approach falls within the category of a moment tensor closure, it does not rely upon an approximation, either analytic or curve fit, of the fourth-moment tensor as do previous closures. This closure is orthotropic in the sense of Cintra & Tucker (*J. Rheol.*, vol. 39, 1995, p. 1095), or equivalently, a natural closure in the sense of Verleye & Dupret (*Developments in Non-Newtonian Flow*, 1993, p. 139). The existence of these explicit formulae has been asserted previously, but as far as the authors know, the explicit forms have yet to be published. The formulae involve elliptic integrals, and are valid whenever fibre orientation was isotropic at some point in time. Finally, this paper presents the fast exact closure, a fast and in principle exact method for solving Jeffery's equation, which does not require approximate closures nor the elliptic integral computation.

Key words: particle/fluid flow, polymer processing, suspensions

1. Introduction

Jeffery's equation (Jeffery 1923) concerns the motion of the direction of an axisymmetric rigid body (henceforth referred to as a fibre) under the influence of a Stokesian fluid whose velocity field is $\boldsymbol{u} = \boldsymbol{u}(\boldsymbol{x}, t)$, and under the assumption that the size of the fibre is infinitesimal compared to any deviations of the flow from its local linear approximation. If $\boldsymbol{p}$ is the unit vector along the axis of symmetry of the fibre which is following the fluid, then it obeys the equation

$$\dot{\boldsymbol{p}} = \boldsymbol{\Omega} \cdot \boldsymbol{p} + \lambda \boldsymbol{E} \cdot \boldsymbol{p} - \lambda \boldsymbol{E} : \boldsymbol{ppp}. \tag{1.1}$$

Here $\boldsymbol{\Omega}$ is the vorticity tensor, that is the anti-symmetric part $\frac{1}{2}(\nabla \boldsymbol{u} - (\nabla \boldsymbol{u})^{\mathrm{T}})$ of the Jacobian of the velocity field $\nabla \boldsymbol{u} = (\partial u_i / \partial x_j)_{1 \leqslant i,j \leqslant 3}$, and $\boldsymbol{E}$ is the rate of strain tensor, that is the symmetric part $\frac{1}{2}(\nabla \boldsymbol{u} + (\nabla \boldsymbol{u})^{\mathrm{T}})$ of the Jacobean of the velocity field.

This is commonly extended to a formula for the fibre orientation distribution $\psi = \psi(\boldsymbol{x}, \boldsymbol{p}, t)$, where $\boldsymbol{p}$ is an element of the two-dimensional sphere S. Thus, given

† Email address for correspondence: david_jack@baylor.edu

https://doi.org/10.1017/jfm.2011.165 Published online by Cambridge University Press

a subset E of S, the proportion of fibres whose direction is in E is given by $\int_E \psi(\boldsymbol{x}, \boldsymbol{p}, t)\,\mathrm{d}\boldsymbol{p}$, where $\mathrm{d}\boldsymbol{p}$ represents the usual integration over S. In particular, an isotropic distribution is represented by $\psi = 1/4\pi$. Then Jeffery's equation for the fibre orientation distribution is

$$\frac{\mathrm{D}}{\mathrm{D}t}\psi = -\nabla_{\boldsymbol{p}} \cdot (\dot{\boldsymbol{p}}\psi), \tag{1.2}$$

where $\mathrm{D}/\mathrm{D}t$ represents the material derivative $\partial/\partial t + \boldsymbol{u}\cdot\nabla$. Equation (1.2) often includes a rotary diffusivity term to account for particle interaction, but that study is left for a related work in Montgomery-Smith, Jack & Smith (2011).

Since (1.2) is, in effect, a partial differential equation in five spatial dimensions, calculating this numerically can be a rather daunting task. Hence, Hinch & Leal (1976) suggested to recast the equation in terms of the higher-order moment tensors. For example, the second and fourth moment tensors are given by

$$\boldsymbol{A} = \int_S \boldsymbol{pp}\psi\,\mathrm{d}\boldsymbol{p}, \qquad \mathbb{A} = \int_S \boldsymbol{pppp}\psi\,\mathrm{d}\boldsymbol{p}. \tag{1.3}$$

Then Jeffery's equation for the second-order moment tensor is

$$\frac{\mathrm{D}}{\mathrm{D}t}\boldsymbol{A} = \boldsymbol{\Omega}\cdot\boldsymbol{A} - \boldsymbol{A}\cdot\boldsymbol{\Omega} + \lambda(\boldsymbol{E}\cdot\boldsymbol{A} + \boldsymbol{A}\cdot\boldsymbol{E}) - 2\lambda\mathbb{A} : \boldsymbol{E}. \tag{1.4}$$

The difficulty with this equation is that it involves the fourth-order moment tensor. To circumvent this problem, various authors (see e.g. Hinch & Leal 1976; Altan *et al.* 1989, 1990; Verleye & Dupret 1993; Cintra & Tucker 1995; VerWeyst *et al.* 1999; Chung & Kwon 2002; Han & Im 2002; Jack & Smith 2005; Jack, Schache & Smith 2010) have proposed *closures*, that is formulae to calculate the fourth-order moment tensor $\mathbb{A}$ from the second-order moment tensor $\boldsymbol{A}$. Many of the approximate closures involve coefficients obtained by fitting numerical data found by solving (1.2) using a finite-element method (see e.g. Bay 1991).

Verleye & Dupret (1993) proposed the *natural closure*. If there was an exact formula for the closure, then it must be the case that the formula is of the form

$$\mathbb{A} = \sum_{0\leqslant m\leqslant n\leqslant 2} \beta_{mn}\mathscr{S}(\boldsymbol{A}^m \otimes \boldsymbol{A}^n). \tag{1.5}$$

Here $\boldsymbol{A}^n$ denotes the matrix power, that is the matrix $\boldsymbol{A}$ multiplied by itself n times, and $\mathscr{S}$ represents the symmetrization of a rank-four tensor, that is

$$\mathscr{S}(\mathbb{B})_{i_1i_2i_3i_4} = \frac{1}{24}\sum_{\sigma} \mathbb{B}_{i_{\sigma_1}i_{\sigma_2}i_{\sigma_3}i_{\sigma_4}}, \tag{1.6}$$

where the sum is over all permutations $\sigma = (\sigma_1, \sigma_2, \sigma_3, \sigma_4)$ of $(1, 2, 3, 4)$. Furthermore, β_{mn} are symmetric functions of the eigenvalues of $\boldsymbol{A}$, or equivalently, functions of the three invariants of $\boldsymbol{A}$, that is, the coefficients of the characteristic polynomial of $\boldsymbol{A}$, which are the trace of $\boldsymbol{A}$, the trace of the adjoint of $\boldsymbol{A}$ and the determinant of $\boldsymbol{A}$. The fact that m and n need only sum up to 2 follows from the Cayley–Hamilton theorem.

Cintra & Tucker (1995) proposed the *orthotropic closure* (ORT). If there was an exact formula for the closure, then it must be the case that if $\boldsymbol{A}$ is diagonal, then $\mathbb{A}_{ijkl}$ must be zero if any index is repeated an odd number of times, and otherwise depend

https://doi.org/10.1017/jfm.2011.165 Published online by Cambridge University Press

only on the diagonal entries of $\boldsymbol{A}$ in such a manner that

$$\mathbb{A}_{1111}(\boldsymbol{A}_{11}, \boldsymbol{A}_{22}, \boldsymbol{A}_{33}) = \mathbb{A}_{1111}(\boldsymbol{A}_{11}, \boldsymbol{A}_{33}, \boldsymbol{A}_{22}), \tag{1.7a}$$

$$\mathbb{A}_{1122}(\boldsymbol{A}_{11}, \boldsymbol{A}_{22}, \boldsymbol{A}_{33}) = \mathbb{A}_{1122}(\boldsymbol{A}_{22}, \boldsymbol{A}_{11}, \boldsymbol{A}_{33}), \tag{1.7b}$$

$$\mathbb{A}_{2222}(\boldsymbol{A}_{11}, \boldsymbol{A}_{22}, \boldsymbol{A}_{33}) = \mathbb{A}_{1111}(\boldsymbol{A}_{22}, \boldsymbol{A}_{11}, \boldsymbol{A}_{33}), \tag{1.7c}$$

$$\mathbb{A}_{3333}(\boldsymbol{A}_{11}, \boldsymbol{A}_{22}, \boldsymbol{A}_{33}) = \mathbb{A}_{1111}(\boldsymbol{A}_{33}, \boldsymbol{A}_{11}, \boldsymbol{A}_{22}), \tag{1.7d}$$

$$\mathbb{A}_{1133}(\boldsymbol{A}_{11}, \boldsymbol{A}_{22}, \boldsymbol{A}_{33}) = \mathbb{A}_{1122}(\boldsymbol{A}_{11}, \boldsymbol{A}_{33}, \boldsymbol{A}_{22}), \tag{1.7e}$$

$$\mathbb{A}_{2233}(\boldsymbol{A}_{11}, \boldsymbol{A}_{22}, \boldsymbol{A}_{33}) = \mathbb{A}_{1122}(\boldsymbol{A}_{22}, \boldsymbol{A}_{33}, \boldsymbol{A}_{11}). \tag{1.7f}$$

They set

$$\mathbb{A}_{1111}(\boldsymbol{A}_{11}, \boldsymbol{A}_{22}, \boldsymbol{A}_{33}) = f(\boldsymbol{A}_{11}, \boldsymbol{A}_{22}, \boldsymbol{A}_{33}), \tag{1.8a}$$

$$\mathbb{A}_{2222}(\boldsymbol{A}_{11}, \boldsymbol{A}_{22}, \boldsymbol{A}_{33}) = g(\boldsymbol{A}_{11}, \boldsymbol{A}_{22}, \boldsymbol{A}_{33}), \tag{1.8b}$$

$$\mathbb{A}_{3333}(\boldsymbol{A}_{11}, \boldsymbol{A}_{22}, \boldsymbol{A}_{33}) = h(\boldsymbol{A}_{11}, \boldsymbol{A}_{22}, \boldsymbol{A}_{33}), \tag{1.8c}$$

when $\boldsymbol{A}_{11} \geqslant \boldsymbol{A}_{22} \geqslant \boldsymbol{A}_{33}$, and then searched for the three functions $f(x, y, z)$, $g(x, y, z)$ and $h(x, y, z)$. They were then able to compute $\mathbb{A}_{1122}$, etc., using the relationship $\sum_i \mathbb{A}_{iijk} = \boldsymbol{A}_{jk}$.

As noted in Cintra & Tucker (1995), since they come from identical assumptions, the natural closure and the orthotropic closure must be theoretically identical, in that β_{mn} must be uniquely determinable from $\mathbb{A}_{iijj}$ and vice versa. This can be seen explicitly by assuming that $\boldsymbol{A}$ is diagonal in (1.5) and seeing that this creates six equations. The transformation from the natural closure to the orthotropic closure is immediate. The converse transformation is seen by solving the six equations for the six unknowns β_{mn}. Calculation shows that the resulting six-by-six matrix is invertible if and only if the diagonal entries of $\boldsymbol{A}$ are distinct. If any of them are repeated, then β_{mn} can be obtained by a limiting process. This suggests that while the natural and orthotropic closures are mathematically equivalent, and that numerically the orthotropic closure will be more stable when any of the eigenvalues of $\boldsymbol{A}$ are repeated, and indeed numerical experiments seem to reveal this.

Verleye & Dupret (1993) noted that indeed there is an exact closure, in the particular case that the fibre orientation distribution is at some time isotropic. Throughout this paper, this will be the standing assumption, unless otherwise stated.

Their exact closure followed from an exact solution to Jeffery's equation in the particular case provided by Dinh & Armstrong (1984) and Lipscomb *et al.* (1988). Verleye & Dupret (1993) gave explicit formulae in the two-dimensional case (see also Altan & Tang 1993, who independently performed the same calculations), but cited an article in preparation for the three-dimensional case, merely noting that the calculations involved elliptic integrals.

VerWeyst (1998) indicated similar exact calculations, citing a personal communication with E. D. Wetzel. Wetzel (1999) provides calculations for a different but related problem and gives solution in terms of elliptic integrals. Therefore, we are somewhat certain that he also obtained the formulae from Verleye & Dupret (1993).

However, neither Dupret, Verleye, VerWeyst nor Wetzel seem to have published their calculations. The traditional approach is to perform these calculations using

https://doi.org/10.1017/jfm.2011.165 Published online by Cambridge University Press

spherical coordinates and the Legendre form of elliptic integrals. However, we use Cartesian coordinates on the sphere (which we assume embedded in the three-dimensional Euclidean space) and the Carlson form of the elliptic integrals. As such, it is quite possible that our formulae are more compact than those obtained. Also, the approach taken here can be easily generalized to other spatial dimensions, should the need arise.

Our analysis also yields what we shall call the fast exact closure (FEC), a rather fast method of solving Jeffery's equation. This method calculates $\mathbb{A}$ by neither using approximate closures nor computing elliptic integrals, but rather by computing an ancillary quantity $\boldsymbol{B}$, which is easily computed via an ordinary differential equation (ODE).

The main contribution of this paper is to explicitly write out the exact formulae (2.7) and (2.10), which as far as we know have not been published elsewhere. A further contribution of this paper is the FEC, which is somewhat muted since this is only valid for Jeffery's equation without the additional rotary diffusion terms. We will amend this in another paper (Montgomery-Smith *et al.* 2011).

Finally, we note that some of the earlier publications asserted that these formulae exist only in the case $\lambda = 1$. However, following Lipscomb *et al.* (1988), it was realized that this restriction is unnecessary.

2. The exact formulae

According to Bretherton (1962), (1.1) can be solved by $\boldsymbol{p} = \boldsymbol{q}/|\boldsymbol{q}|$, where $\boldsymbol{q}$ satisfies

$$\dot{\boldsymbol{q}} = (\boldsymbol{\Omega} + \lambda \boldsymbol{E}) \cdot \boldsymbol{q}. \tag{2.1}$$

This can be seen by simple substitution. Consequently, it was found by Dinh & Armstrong (1984) (for the case $\lambda = 1$) and Lipscomb *et al.* (1988), and later Szeri & Lin (1996), that if the fibre orientation distribution is initially isotropic, that is $\psi = 1/4\pi$ at $t = 0$, then the solution to (1.2) is

$$\psi(\boldsymbol{p}) = \frac{1}{4\pi(\boldsymbol{B} : \boldsymbol{pp})^{3/2}}. \tag{2.2}$$

Here $\boldsymbol{B} = \boldsymbol{C}^{\mathrm{T}}\boldsymbol{C}$, where $\boldsymbol{C}$ satisfies

$$\frac{\mathrm{D}}{\mathrm{D}t}\boldsymbol{C} = -\boldsymbol{C} \cdot (\boldsymbol{\Omega} + \lambda \boldsymbol{E}), \quad \boldsymbol{C} = \boldsymbol{I} \text{ at } t = 0, \tag{2.3}$$

or equivalently that $\boldsymbol{B}$ satisfies

$$\frac{\mathrm{D}}{\mathrm{D}t}\boldsymbol{B} = -\boldsymbol{B} \cdot (\boldsymbol{\Omega} + \lambda \boldsymbol{E}) - (-\boldsymbol{\Omega} + \lambda \boldsymbol{E}) \cdot \boldsymbol{B}, \quad \boldsymbol{B} = \boldsymbol{I} \text{ at } t = 0. \tag{2.4}$$

We also note that (2.2) generalizes as follows: if $\psi = \psi_0$ at $t = 0$,

$$\psi(\boldsymbol{p}) = \frac{\psi_0(\boldsymbol{C} \cdot \boldsymbol{p}/|\boldsymbol{C} \cdot \boldsymbol{p}|)}{(\boldsymbol{B} : \boldsymbol{pp})^{3/2}}. \tag{2.5}$$

For the purposes of the exact closure, the precise nature of $\boldsymbol{B}$ is not required. All that is necessary to know is that $\boldsymbol{B}$ is a positive definite matrix with determinant one.

https://doi.org/10.1017/jfm.2011.165 Published online by Cambridge University Press

From the definition in (1.3) along with (2.2), the formula for the second-order moment tensor may be expressed as

$$\boldsymbol{A} = \int_S \frac{\boldsymbol{pp}}{4\pi(\boldsymbol{B} : \boldsymbol{pp})^{3/2}}\,\mathrm{d}\boldsymbol{p}. \tag{2.6}$$

Verleye & Dupret assert, without proof but somewhat reasonably, that this provides a one-to-one correspondence between positive definite matrices $\boldsymbol{B}$ with determinant one, and positive definite matrices $\boldsymbol{A}$ with trace one. By inverting the formula in (2.6), one obtains a formula for $\boldsymbol{B}$ in terms of $\boldsymbol{A}$. We present the complete proof in the Appendix showing that this expression provides a one-to-one and onto relationship between $\boldsymbol{A}$ and $\boldsymbol{B}$.

The integral in (2.6) is not sufficient for rapid computations, and we change the expression into the integral formula (see the derivation in the Appendix)

$$\boldsymbol{A} = \frac{1}{2}\int_0^\infty \frac{(\boldsymbol{B} + s\boldsymbol{I})^{-1}\,\mathrm{d}s}{\sqrt{\det(\boldsymbol{B} + s\boldsymbol{I})}}. \tag{2.7}$$

To perform this calculation numerically, diagonalize $\boldsymbol{B}$ with an orthogonal matrix. Then $\boldsymbol{A}$ is transformed to a diagonal matrix via exactly the same similarity matrix and (2.7) becomes

$$\boldsymbol{A}_{11} = \frac{1}{2}\int_0^\infty \frac{\mathrm{d}s}{(b_1+s)^{3/2}\sqrt{b_2+s}\sqrt{b_3+s}}, \tag{2.8a}$$

$$\boldsymbol{A}_{22} = \frac{1}{2}\int_0^\infty \frac{\mathrm{d}s}{\sqrt{b_1+s}(b_2+s)^{3/2}\sqrt{b_3+s}}, \tag{2.8b}$$

$$\boldsymbol{A}_{33} = \frac{1}{2}\int_0^\infty \frac{\mathrm{d}s}{\sqrt{b_1+s}\sqrt{b_2+s}(b_3+s)^{3/2}}, \tag{2.8c}$$

where b_1, b_2 and b_3 are the diagonal entries of $\boldsymbol{B}$. These integrals are one-third the r_D Carlson form of the elliptic integrals (Carlson 1995). The Carlson elliptic integrals have good numerical algorithms to compute them, for example, they are part of the suite of special functions provided by the GNU Scientific Library (2009) and are also described by Press *et al.* (2003). (We refer to the elliptic integrals as the Carlson form, because that is how it appears in Press *et al.* 2003. However, such integrals appeared far earlier in the study of external ellipsoid harmonics, see for example Oberbeck 1876, Hobson 1931 and Jeffery 1923.)

Combining (1.3) and (2.6), the fourth-order moment tensor may be expressed as

$$\mathbb{A} = \int_S \frac{\boldsymbol{pppp}}{4\pi(\boldsymbol{B} : \boldsymbol{pp})^{3/2}}\,\mathrm{d}\boldsymbol{p}, \tag{2.9}$$

where we demonstrate in the Appendix that this form may be transformed into

$$\mathbb{A} = \frac{3}{4}\int_0^\infty \frac{s\,\mathscr{S}((\boldsymbol{B} + s\boldsymbol{I})^{-1} \otimes (\boldsymbol{B} + s\boldsymbol{I})^{-1})\,\mathrm{d}s}{\sqrt{\det(\boldsymbol{B} + s\boldsymbol{I})}}, \tag{2.10}$$

https://doi.org/10.1017/jfm.2011.165 Published online by Cambridge University Press

or in the special case that $\boldsymbol{B}$ is diagonal (or equivalently when $\boldsymbol{A}$ is diagonal) can be computed via the equations

$$\mathbb{A}_{1111} = \frac{3}{4}\int_0^\infty \frac{s\,\mathrm{d}s}{(b_1+s)^{5/2}\sqrt{b_2+s}\sqrt{b_3+s}}, \tag{2.11a}$$

$$\mathbb{A}_{2222} = \frac{3}{4}\int_0^\infty \frac{s\,\mathrm{d}s}{\sqrt{b_1+s}(b_2+s)^{5/2}\sqrt{b_3+s}}, \tag{2.11b}$$

$$\mathbb{A}_{3333} = \frac{3}{4}\int_0^\infty \frac{s\,\mathrm{d}s}{\sqrt{b_1+s}\sqrt{b_2+s}(b_3+t)^{5/2}}, \tag{2.11c}$$

$$\mathbb{A}_{1122} = \frac{1}{4}\int_0^\infty \frac{s\,\mathrm{d}s}{(b_1+s)^{3/2}(b_2+s)^{3/2}\sqrt{b_3+s}}, \tag{2.11d}$$

$$\mathbb{A}_{1133} = \frac{1}{4}\int_0^\infty \frac{s\,\mathrm{d}s}{(b_1+s)^{3/2}\sqrt{b_2+s}(b_3+s)^{3/2}}, \tag{2.11e}$$

$$\mathbb{A}_{2233} = \frac{1}{4}\int_0^\infty \frac{s\,\mathrm{d}s}{\sqrt{b_1+s}(b_2+s)^{3/2}(b_3+s)^{3/2}}, \tag{2.11f}$$

all the other coefficients of $\mathbb{A}$ being zero. When the eigenvalues of $\boldsymbol{B}$ are distinct, these can be computed by the easily derived formulae

$$\mathbb{A}_{1122} = \frac{b_1\boldsymbol{A}_{11} - b_2\boldsymbol{A}_{22}}{2(b_1-b_2)}, \tag{2.12a}$$

$$\mathbb{A}_{1133} = \frac{b_1\boldsymbol{A}_{11} - b_3\boldsymbol{A}_{33}}{2(b_1-b_3)}, \tag{2.12b}$$

$$\mathbb{A}_{2233} = \frac{b_2\boldsymbol{A}_{22} - b_3\boldsymbol{A}_{33}}{2(b_2-b_3)}, \tag{2.12c}$$

$$\mathbb{A}_{1111} = \boldsymbol{A}_{11} - \mathbb{A}_{1122} - \mathbb{A}_{1133}, \tag{2.12d}$$

$$\mathbb{A}_{2222} = \boldsymbol{A}_{22} - \mathbb{A}_{1122} - \mathbb{A}_{2233}, \tag{2.12e}$$

$$\mathbb{A}_{3333} = \boldsymbol{A}_{33} - \mathbb{A}_{1133} - \mathbb{A}_{2233}. \tag{2.12f}$$

If two of the eigenvalues are close to each other, for example $b_1 = b_2 + \epsilon$, then (2.12) will give division by zero errors or at least large numerical errors. However, we see from (2.11) that $\boldsymbol{A}_{1111} + \boldsymbol{A}_{2222} = 6\boldsymbol{A}_{1122} + O(\epsilon^2)$, and hence

$$\mathbb{A}_{1133} = \frac{b_1\boldsymbol{A}_{11} - b_3\boldsymbol{A}_{33}}{2(b_1-b_3)}, \tag{2.13a}$$

$$\mathbb{A}_{2233} = \frac{b_2\boldsymbol{A}_{22} - b_3\boldsymbol{A}_{33}}{2(b_2-b_3)}, \tag{2.13b}$$

$$\mathbb{A}_{1122} = \frac{1}{8}(\boldsymbol{A}_{11} + \boldsymbol{A}_{22} - \mathbb{A}_{1133} - \mathbb{A}_{2233}) + O(\epsilon^2), \tag{2.13c}$$

$$\mathbb{A}_{1111} = \boldsymbol{A}_{11} - \mathbb{A}_{1122} - \mathbb{A}_{1133}, \tag{2.13d}$$

$$\mathbb{A}_{2222} = \boldsymbol{A}_{22} - \mathbb{A}_{1122} - \mathbb{A}_{2233}, \tag{2.13e}$$

$$\mathbb{A}_{3333} = \boldsymbol{A}_{33} - \mathbb{A}_{1133} - \mathbb{A}_{2233}, \tag{2.13f}$$

where similar forms exist when $b_1 = b_3 + \epsilon$ or $b_2 = b_3 + \epsilon$. If all three of the eigenvalues are almost equal, that is $b_1 = 1 + c_1$, $b_2 = 1 + c_2$, $b_3 = 1 + c_3$ with $c_1, c_2, c_3 = O(\epsilon)$ (so

https://doi.org/10.1017/jfm.2011.165 Published online by Cambridge University Press

necessarily $c_1 + c_2 + c_3 = O(\epsilon^2)$),

$$\mathbb{A}_{1111} = \frac{1}{5} - \frac{3}{14}c_1 - \frac{3}{70}c_2 - \frac{3}{70}c_3 + O(\epsilon^2), \tag{2.14a}$$

$$\mathbb{A}_{2222} = \frac{1}{5} - \frac{3}{70}c_1 - \frac{3}{14}c_2 - \frac{3}{70}c_3 + O(\epsilon^2), \tag{2.14b}$$

$$\mathbb{A}_{3333} = \frac{1}{5} - \frac{3}{70}c_1 - \frac{3}{70}c_2 - \frac{3}{14}c_3 + O(\epsilon^2), \tag{2.14c}$$

$$\mathbb{A}_{1122} = \frac{1}{15} - \frac{3}{70}c_1 - \frac{3}{70}c_2 - \frac{1}{70}c_3 + O(\epsilon^2), \tag{2.14d}$$

$$\mathbb{A}_{1133} = \frac{1}{15} - \frac{3}{70}c_1 - \frac{1}{70}c_2 - \frac{3}{70}c_3 + O(\epsilon^2), \tag{2.14e}$$

$$\mathbb{A}_{2233} = \frac{1}{15} - \frac{1}{70}c_1 - \frac{3}{70}c_2 - \frac{3}{70}c_3 + O(\epsilon^2). \tag{2.14f}$$

For example, assuming that the ODE solver is accurate to n digits, it is appropriate to use (2.13) or (2.14) if any of the eigenvalues of $\boldsymbol{B}$ have a relative difference bounded by about $10^{-n/3}$. The resulting $\mathbb{A}$ should then be accurate to about $2n/3$ digits. We expect the loss of precision is unlikely to have a large effect on the final solution, because the event when $\boldsymbol{B}$ has eigenvalues close to each other occurs somewhat rarely, and these events will largely be integrated by (2.4).

The exact closure can be summarized by first diagonalizing $\boldsymbol{A}$, then computing $\boldsymbol{B}$ by inverting formulae (2.8), then computing $\mathbb{A}$ using (2.11), and finally using the inverse of the similarity matrix from the diagonalization of $\boldsymbol{A}$ to transform $\mathbb{A}$. To compute formulae (2.11), use (2.12), (2.13) or (2.14), as appropriate.

These numerical calculations will necessarily take some time to perform (particularly the inversion process which requires a multidimensional root finding). VerWeyst (1998) described a different process where these formulae were used to generate values which were then fitted to polynomial approximations to the functions f, g and h as in (1.8).

3. The fast exact closure

Our analysis yields another method for solving Jeffery's equation, with the proviso that the probability distribution was isotropic at some time in its history where the goal is to solve (1.4). The difficulty of finding $\boldsymbol{B}$ can be solved by simultaneously solving (2.4) along with (1.4). During this process, $\mathbb{A}$ can be calculated using (2.12)–(2.14). In this way, an exact solution is obtained, without the need to compute the elliptic integrals.

The only difficulty lies in the initial data. If the data are isotropic, one simply sets $\boldsymbol{A} = \frac{1}{3}\boldsymbol{I}$ and $\boldsymbol{B} = \boldsymbol{I}$ at $t = 0$. Conversely, if the initial data are not isotropic, then the initial data for $\boldsymbol{B}$ can be calculated by inverting (2.7). This can be performed by diagonalizing $\boldsymbol{A}$, computing $\boldsymbol{B}$ by inverting (2.8) and then reversing the change of basis that was used to diagonalize $\boldsymbol{A}$. While this calculation could conceivably be quite slow, as the inversion of (2.8) will require a three-dimensional root-finding method as well as computing the elliptic integrals, which needs to be performed only for the initial step.

This method should run at about the same speed as computing the orthotropic closure algorithms of Cintra & Tucker (1995) and VerWeyst *et al.* (1999). The workload of this algorithm involves solving an ordinary differential equation in about 11 variables, where the main computational effort will be to diagonalize the matrices and perform

https://doi.org/10.1017/jfm.2011.165 Published online by Cambridge University Press

the change of basis for the rank-two and rank-four tensors. (Note that $\boldsymbol{A}$ and $\boldsymbol{B}$ will be simultaneously diagonalizable, that is the orthogonal matrix used to diagonalize one of the second-order tensors can and should be used to diagonalize the other.)

A major problem with the FEC is that it only works in the case when there is no rotary diffusion term. However, the pure Jeffery's equation without a rotary diffusion term is applicable only to a single fibre in a fluid, and so is unrealistic. Resolving this issue is a major extension of this paper, and we address this in a future paper (Montgomery-Smith *et al.* 2011).

4. Behaviour of the fast exact closure

Direct solutions of tensor $\boldsymbol{C}$ of (2.3) will serve as the basis upon which to compare the effectiveness of the FEC. The transient solution of $\boldsymbol{C}$ in (2.3), assuming constant velocity gradients, is given by

$$\boldsymbol{C} = \exp(-t(\boldsymbol{\Omega} + \lambda \boldsymbol{E})), \tag{4.1}$$

where 'exp' denotes the matrix exponential. The solution for $\boldsymbol{B}$ readily follows from the definition $\boldsymbol{B} = \boldsymbol{C}^{\mathrm{T}}\boldsymbol{C}$ from the solution of $\boldsymbol{C}$ in (2.3), and the second-order orientation tensor $\boldsymbol{A}$ is obtained from (2.6). This solution approach, which we term the analytic solution, is not only effective for flows originating from an isotropic initial condition with constant velocity gradients but will also serve as the basis upon which to compare results from various closures which numerically solve the equation of motion for the orientation tensor $\boldsymbol{A}$ of (1.4).

To demonstrate the effectiveness of the FEC, solutions are compared to results from several popular closures, the quadratic (Doi 1981), the hybrid (Advani & Tucker 1987) and the ORT (VerWeyst 1998; VerWeyst & Tucker 2002), and all results will be compared to the analytic solutions from (4.1). The three comparison closures are selected based on their common employment in industrial simulations of fibre orientation (e.g. the quadratic and the hybrid) and their known accuracy (e.g. the ORT). It is expected the ORT closure's accuracy will be quite high considering it is based off of similar 'exact' calculations (VerWeyst 1998) to the FEC. The ORT is known to give similar results to the invariant-based optimal fitting (IBOF) closure of Chung & Kwon (2002), which is an extension of the natural closure discussed by Verleye & Dupret (1993). Solutions for the existing closures (quadratic, hybrid or ORT) are performed by solving (1.4) and using the respective closure to approximate $\mathbb{A}$ in terms of $\boldsymbol{A}$.

The simple shear flow considered ($\boldsymbol{v} = [Gx_3, 0, 0]^{\mathrm{T}}$, where G is the scalar magnitude of the rate of deformation $G = ||\boldsymbol{E}||$) begins from an initial isotropic orientation (i.e. $\psi = 1/4\pi$). The primary reason for choosing a pure shearing flow is twofold. The first, and primary, reason is the prevalence of shearing-dominated flows in industrial injection molding processes. An alternative, yet more constraining, motivation for choosing a pure shearing flow is to demonstrate the FEC's ability to capture the correct period for the Jeffery orbit. It is this oscillatory nature of the orientation in pure Jeffery's motion that causes significant numerical difficulties for classical approaches that rely on alternative methods such as finite differences (Bay & Tucker 1991; Bay 1991) or the spherical harmonic expansion approach (see e.g. Bird, Armstrong & Hassager 1987; Montgomery-Smith, Jack & Smith 2010). It is worthwhile to note that the interior of the eigenspace triangle containing all possible orientations (see e.g. Cintra & Tucker 1995 for a full discussion) with an initial isotropic orientation state can only be populated by shearing flows, whereas orientations occurring on the boundaries are caused by pure elongational flows and will have two repeated eigenvalues of $\boldsymbol{A}$ and $\boldsymbol{B}$.

https://doi.org/10.1017/jfm.2011.165 Published online by Cambridge University Press

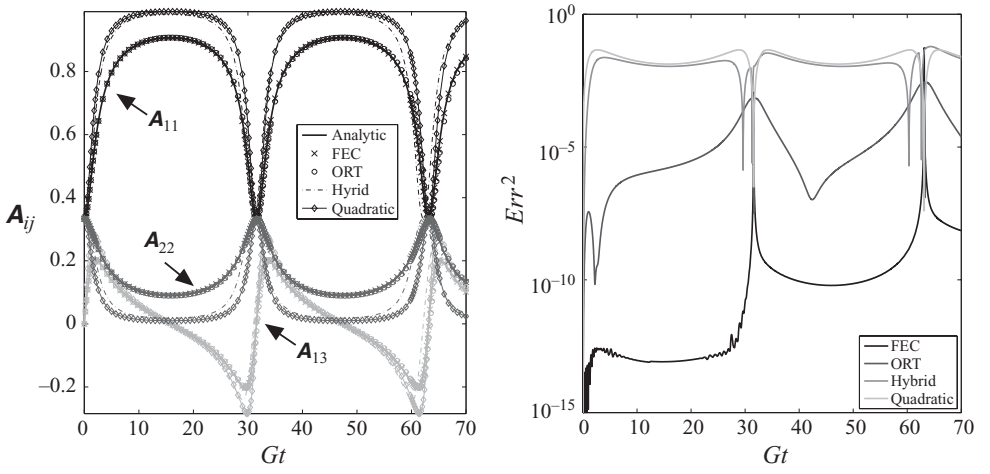


FIGURE 1. Plot of $\boldsymbol{A}_{11}$ for simple shear flow with $\lambda = 0.98$ from various closures along with the associated error Err.

Solutions of pure shear flow are run for the orientation parameter $\lambda = 0.98$, which corresponds to a fibre aspect ratio of $a_r = L/d \simeq 9.95$. The results for the second-order orientation tensor $\boldsymbol{A}$ from each solution approach are given in figure 1 and compared to direct computations of the analytic solution of (4.1) for tensor $\boldsymbol{C}$ and then using the elliptic integral relationship of (2.8) to obtain $\boldsymbol{A}$. As observed in the figure, the periodic nature of the orientation solution of $\boldsymbol{A}_{ij}$ is captured reasonably by each of the solution approaches. An ellipsoid experiencing Jeffery motion in a pure shearing flow will rotate with a period, τ, of (Jeffery 1923)

$$\tau = \frac{2\pi}{||\boldsymbol{E}||\sqrt{(1-\lambda^2)}}, \tag{4.2}$$

where the solution of (4.2) may be obtained by analysing the eigenvalues of $\boldsymbol{\Omega} + \lambda \boldsymbol{E}$ from (2.1). In our example, $\lambda = 0.98$ and $||\boldsymbol{E}|| = G$ and thus $\tau = 31.574/G$. This period can be observed by noting a particular orientation condition, and tabulating the time it takes to return to the same orientation state. Since there are numerical errors introduced by the numerical solution of a system of ODEs with a periodic solution, returning to the numerically identical orientation state may never occur. Thus, we compare the initial isotropic orientation with that occurring near where the three eigenvalues are nearest to each other and can approximate the period of the numerical solution for pure show flow through the expression

$$\tau_{closure} = t \text{ such that } |a_1 - a_3| \text{ is minimized over } Gt \in [30, 33], \tag{4.3}$$

where a_1, a_2 and a_3 are the eigenvalues of the second-order orientation tensor $\boldsymbol{A}$ in descending order, $a_1 \geqslant a_2 \geqslant a_3 \geqslant 0$. Therefore, the orientation from the numerical solutions employing closures will be closest to isotropic ($a_1 = a_2 = a_3 = 1/3$) when $a_1 \simeq a_3$. The FEC, ORT, hybrid and quadratic closures have observed periods of respectively $G\tau_{FEC} = 31.572$, $G\tau_{ORT} = 31.708$, $G\tau_{hybrid} = 31.081$ and $G\tau_{quadratic} = 31.575$. Each closure is reasonably accurate, whereas the FEC and quadratic closures are the most effective in representing the actual period. However, by observing the orientation path taken by each closure, the quadratic and the hybrid closures are clearly ineffective in predicting the orientation state during most of the

https://doi.org/10.1017/jfm.2011.165 Published online by Cambridge University Press

flow history. The FEC and ORT closures follow the analytic solution quite well. To aid the comparison between closures, the error plotted in figure 1 is defined as the difference in the eigenvalues from the analytic solution and the numeric solution from the closures as

$$Err^2 = \sum_{i=1}^{2} \left(a_i^{analytic} - a_i^{closure}\right)^2. \tag{4.4}$$

The value of Err shows the effectiveness of a closure in conjunction with the solution of the ODEs in (1.4) and (2.4) and where it has the greatest deviation in the orientation solution. It is interesting to note that the FEC performs quite well throughout much of the flow history. This characteristic is true, except when the orientation approaches isotropic. This is not unexpected due to the nature of the closure since this is where the eigenvalues of $\boldsymbol{A}$ all approach the same value of 1/3 and the approximation of (2.14) must be accepted due to the aforementioned numerical limitations of repeated eigenvalues. It is worthwhile to note that both the ORT and the FEC yield solutions that are a considerable improvement over the commonly employed quadratic and hybrid closures, which for the ORT is not surprising and this characteristic has been widely discussed in the literature. It should not be intended to infer that the FEC is proposed as an improvement over the quite sufficient ORT closure, where the accuracy to the third decimal place observed by the ORT closure is considered quite acceptable in injection molding predictions (see e.g. Chung & Kwon 2002), but the FEC serves as a starting point for the development of a new class of closures for fibre systems with colliding particles which add a diffusion term to (1.2) (see e.g. Montgomery-Smith *et al.* 2010 for a listing of existing diffusion models). For the industrially applicable case of concentrated suspensions of fibres, extensions to the FEC have been performed by Montgomery-Smith *et al.* (2011) for Jeffery's equation with rotary diffusion.

The authors have performed similar studies for flows beyond pure shear and the results and conclusions for virtually all flows are identical to those from simple shear. It is expected that flows with repeated eigenvalues (i.e. orientations occurring on the boundaries of the eigenspace triangle containing all physically possible orientations discussed in Cintra & Tucker 1995) would cause problems due to the numerical approximation that must be made in (2.13) or (2.14). However, for flows that have some non-zero shear coupled with elongation, as would be expected in virtually all industrial flows, the FEC and the ORT closures both perform quite well and the aforementioned conclusions for the accuracy and stability for pure shear were equivalent for all flows investigated with mixed shearing and uniaxial elongation. The primary difference between the pure shear flow and the shear-elongation flow is the absence of any periodic behaviour due to the elongation, and thus the numerical issues in the ODE solution are greatly diminished as $t \to \infty$. It is noted that coupled flows with shearing and biaxial elongation were also performed, and for cases when biaxial elongation dominated the flow, numerical instabilities were observed in the FEC since $a_1 \simeq a_2$ remains true throughout the entire flow history. This case is worthwhile to recognize, but is not of a significant concern as this orientation state will rarely, if ever, occur in actual industrial processes.

5. Conclusion

In this paper, we have presented an exact closure, which was at least in part, understood by previous authors. We have found that an analysis of the formulae

https://doi.org/10.1017/jfm.2011.165 Published online by Cambridge University Press

gives rise to the FEC, which exactly solves Jeffery's equation in a fast manner for any orientation that at one point in time was isotropic. This work demonstrates that the observations of previous authors were correct that solutions of the Jeffery's equation must exist. The FEC closure presents a systematic approach to solve the Jeffery's equation while simultaneously solving a related differential equation, thus avoiding both the cumbersome elliptic integral evaluation and the necessity for a closure of a higher-order moment tensor. It is noted that industrial simulations often add in a term like $\boldsymbol{C}_I\|\boldsymbol{E}\|(2\boldsymbol{I}-6\boldsymbol{A})$ to (1.4), and then presume that the closure that creates $\mathbb{A}$ from $\boldsymbol{A}$ is still valid. However, to add diffusion terms to the FEC method requires adding a similar term to (2.4). For the work which explores approximations to versions of Jeffery's equation with diffusion terms added, for example, the Folgar–Tucker equation (Folgar & Tucker 1984), the interested reader is directed towards Montgomery-Smith *et al.* (2011).

The authors gratefully acknowledge support from NSF via grant C.M.M.I. 0727399.

Appendix. Justification of the formulae

First, we show that the initially isotropic orientation distribution function from (2.2) and (2.5) are solutions to (1.2). Even though this is not a new result, we present our proof, first to keep the presentation self-contained and second because we later use the intermediate equation (A 6). However, note that the proof in Szeri & Lin (1996) is superior.

If E is a subset of S, then the proportion of fibres whose direction is contained in E is

$$\int_E \psi(\boldsymbol{p})\,\mathrm{d}\boldsymbol{p} = \frac{4}{\pi^{1/2}}\int_{r=0}^{\infty}\int_{\boldsymbol{p}\in E}\psi(\boldsymbol{p})r^2\,\mathrm{e}^{-r^2}\,\mathrm{d}\boldsymbol{p}\,\mathrm{d}r = \frac{1}{\pi^{3/2}}\int_{\boldsymbol{q}\in\bar{E}}\psi\left(\frac{\boldsymbol{q}}{|\boldsymbol{q}|}\right)\mathrm{e}^{-|\boldsymbol{q}|^2}\,\mathrm{d}\boldsymbol{q}. \quad (A\,1)$$

Here $\bar{E}$ denotes the set of elements $\boldsymbol{q}\in\mathbb{R}^3-\{0\}$ such that $\boldsymbol{q}/|\boldsymbol{q}|\in E$. The first equality follows because $\int_0^\infty r^2\,\mathrm{e}^{-r^2}\,\mathrm{d}r=\pi^{1/2}/4$. The second equality is just the conversion from spherical coordinates to Cartesian coordinates, noting that $4\pi r^2\,\mathrm{d}r\,\mathrm{d}\boldsymbol{p}=\mathrm{d}\boldsymbol{q}$.

Note that (2.1) is solved by setting $\boldsymbol{q}=\boldsymbol{C}^{-1}\cdot\boldsymbol{p}(0)$, where $\boldsymbol{C}$ satisfies (2.3), because $\boldsymbol{C}^{-1}$ satisfies the equation

$$\frac{\mathrm{D}}{\mathrm{D}t}\boldsymbol{C}^{-1} = (\boldsymbol{\Omega}+\lambda\boldsymbol{E})\cdot\boldsymbol{C}^{-1}, \quad \boldsymbol{C}^{-1}=\boldsymbol{I}\text{ at }t=0. \quad (A\,2)$$

Thus, a fibre which at time t is in a direction $\boldsymbol{p}$ originates from a fibre which at time $t=0$ was in the direction $\boldsymbol{p}_0=\boldsymbol{C}\cdot\boldsymbol{p}/|\boldsymbol{C}\cdot\boldsymbol{p}|$. The sets E and $\bar{E}$ originate from the sets $E_0=\{\boldsymbol{C}\cdot\boldsymbol{p}/|\boldsymbol{C}\cdot\boldsymbol{p}| : \boldsymbol{p}\in E\}$ and $\bar{E}_0=\boldsymbol{C}\cdot\bar{E} := \{\boldsymbol{C}\cdot\boldsymbol{q} : \boldsymbol{q}\in\bar{E}\}$, respectively. Thus,

$$\int_E \psi(\boldsymbol{p})\,\mathrm{d}\boldsymbol{p} = \int_{E_0}\psi_0(\boldsymbol{p})\,\mathrm{d}\boldsymbol{p}. \quad (A\,3)$$

Rewriting (A 1) for the time $t=0$, we obtain

$$\int_{\boldsymbol{E}_0}\psi_0(\boldsymbol{p})\,\mathrm{d}\boldsymbol{p} = \pi^{-3/2}\int_{\boldsymbol{q}\in\bar{E}_0}\psi_0\left(\frac{\boldsymbol{q}}{|\boldsymbol{q}|}\right)\mathrm{e}^{-|\boldsymbol{q}|^2}\,\mathrm{d}\boldsymbol{q}. \quad (A\,4)$$

https://doi.org/10.1017/jfm.2011.165 Published online by Cambridge University Press

Performing the change of variables $\boldsymbol{q} \mapsto \boldsymbol{C}\cdot\boldsymbol{q}$, and noting that $\mathrm{d}\boldsymbol{q} = \mathrm{d}(\boldsymbol{C}\cdot\boldsymbol{q})$ (because the determinant of $\boldsymbol{C}$ is one), we obtain

$$\begin{aligned}\int_{\boldsymbol{E}_0} \psi_0(\boldsymbol{p})\,\mathrm{d}\boldsymbol{p} &= \pi^{-3/2}\int_{\boldsymbol{q}\in\bar{E}} \psi_0\left(\frac{\boldsymbol{C}\cdot\boldsymbol{q}}{|\boldsymbol{C}\cdot\boldsymbol{q}|}\right)\mathrm{e}^{-|\boldsymbol{C}\cdot\boldsymbol{q}|^2}\,\mathrm{d}\boldsymbol{q}\\ &= \pi^{-3/2}\int_{\boldsymbol{p}\in E}\int_{r=0}^{\infty} \psi_0\left(\frac{\boldsymbol{C}\cdot\boldsymbol{p}}{|\boldsymbol{C}\cdot\boldsymbol{p}|}\right) r^2\,\mathrm{e}^{-|\boldsymbol{C}\cdot\boldsymbol{p}|^2 r^2}\,\mathrm{d}r\,\mathrm{d}\boldsymbol{p}, \end{aligned} \tag{A 5}$$

where the last equality follows by converting Cartesian coordinates to spherical coordinates. Combining this with (A 1), and noting that these equations work for any subset E of S, we obtain

$$\psi(\boldsymbol{p}) = 4\pi^{-1/2}\psi_0\left(\frac{\boldsymbol{C}\cdot\boldsymbol{p}}{|\boldsymbol{C}\cdot\boldsymbol{p}|}\right)\int_{r=0}^{\infty} r^2\,\mathrm{e}^{-|\boldsymbol{C}\cdot\boldsymbol{p}|^2 r^2}\,\mathrm{d}r = \frac{\psi_0(\boldsymbol{C}\cdot\boldsymbol{p}/|\boldsymbol{C}\cdot\boldsymbol{p}|)}{|\boldsymbol{C}\cdot\boldsymbol{p}|^3} \tag{A 6}$$

as required. Equation (2.2) is an immediate corollary of (2.5).

Next, we show that the transformation of the second-order orientation tensor of (2.7) and (2.8) from (2.6) is valid. Note that if $\boldsymbol{B}$ is diagonal with diagonal entries b_1, b_2, b_3, then from (A 6),

$$\psi(\boldsymbol{p}) = \frac{1}{\pi^{3/2}}\int_0^{\infty} r^2 \exp(-r^2(b_1p_1^2 + b_2p_2^2 + b_3p_3^2))\,\mathrm{d}r. \tag{A 7}$$

By symmetry, we can see that the off-diagonal entries of $\boldsymbol{A}$ are zero and the diagonal entries are computed, for example, by

$$\begin{aligned}\boldsymbol{A}_{11} &= \frac{1}{\pi^{3/2}}\int_S\int_{r=0}^{\infty} r^2p_1^2\exp(-r^2(b_1p_1^2 + b_2p_2^2 + b_3p_3^2))\,\mathrm{d}r\,\mathrm{d}\boldsymbol{p}\\ &= \frac{1}{\pi^{3/2}}\int_{\mathbb{R}^3}\frac{q_1^2}{|\boldsymbol{q}|^2}\exp(-(b_1q_1^2 + b_2q_2^2 + b_3q_3^2))\,\mathrm{d}\boldsymbol{q}. \end{aligned} \tag{A 8}$$

Now, if we set

$$f(s) = \frac{1}{\pi^{3/2}}\int_{\mathbb{R}^3}\frac{q_1^2}{|\boldsymbol{q}|^2}\exp(-((b_1+s)q_1^2 + (b_2+s)q_2^2 + (b_3+s)q_3^2))\,\mathrm{d}\boldsymbol{q}, \tag{A 9}$$

then we see that

$$\begin{aligned} f'(s) &= -\frac{1}{\pi^{3/2}}\int_{\mathbb{R}^3} q_1^2\exp(-((b_1+s)q_1^2 + (b_2+s)q_2^2 + (b_3+s)q_3^2))\,\mathrm{d}\boldsymbol{q}\\ &= -\frac{1}{\pi^{3/2}}\int_{-\infty}^{\infty} q_1^2\,\mathrm{e}^{-(b_1+s)q_1^2}\,\mathrm{d}q_1\int_{-\infty}^{\infty}\mathrm{e}^{-(b_2+s)q_2^2}\,\mathrm{d}q_2\int_{-\infty}^{\infty}\mathrm{e}^{-(b_3+s)q_3^2}\,\mathrm{d}q_3\\ &= -\frac{1}{2(b_1+s)^{3/2}\sqrt{b_2+s}\sqrt{b_3+s}}. \end{aligned} \tag{A 10}$$

Since it is evident that $f(s)\to 0$ as $s\to\infty$, we obtain

$$\boldsymbol{A}_{11} = \frac{1}{2}\int_0^{\infty}\frac{\mathrm{d}s}{(b_1+s)^{3/2}\sqrt{b_2+s}\sqrt{b_3+s}}. \tag{A 11}$$

To show (2.7), it is necessary to consider only the case when $\boldsymbol{B}$ is diagonal, and in this case the formula follows immediately from (2.8).

https://doi.org/10.1017/jfm.2011.165 Published online by Cambridge University Press

Next, we show that the transformation of the fourth-order orientation tensor of (2.10) and (2.11) from (2.9) is valid. We illustrate the argument with the example

$$\begin{aligned}\mathbb{A}_{1111} &= \frac{1}{\pi^{3/2}}\int_S\int_{r=0}^{\infty} r^2 p_1^4 \exp(-r^2(b_1p_1^2+b_2p_2^2+b_3p_3^2))\,\mathrm{d}r\,\mathrm{d}\boldsymbol{p}\\ &= \frac{1}{\pi^{3/2}}\int_{\mathbb{R}^3}\frac{q_1^4}{|\boldsymbol{q}|^4}\exp(-(b_1q_1^2+b_2q_2^2+b_3q_3^2))\,\mathrm{d}\boldsymbol{q}.\end{aligned} \tag{A 12}$$

We set

$$g(s) = \frac{1}{\pi^{3/2}}\int_{\mathbb{R}^3}\frac{q_1^4}{|\boldsymbol{q}|^4}\exp(-((b_1+s)q_1^2+(b_2+s)q_2^2+(b_3+s)q_3^2))\,\mathrm{d}\boldsymbol{q}, \tag{A 13}$$

and see that

$$\begin{aligned}g''(s) &= \frac{1}{\pi^{3/2}}\int_{\mathbb{R}^3} q_1^4\exp(-((b_1+s)q_1^2+(b_2+s)q_2^2+(b_3+s)q_3^2))\,\mathrm{d}\boldsymbol{q}\\ &= \frac{1}{\pi^{3/2}}\int_{-\infty}^{\infty} q_1^4\,\mathrm{e}^{-(b_1+s)q_1^2}\,\mathrm{d}q_1\int_{-\infty}^{\infty}\mathrm{e}^{-(b_2+s)q_2^2}\,\mathrm{d}q_2\int_{-\infty}^{\infty}\mathrm{e}^{-(b_3+s)q_3^2}\,\mathrm{d}q_3\\ &= \frac{3}{4(b_1+s)^{5/2}\sqrt{b_2+s}\sqrt{b_3+s}}\end{aligned} \tag{A 14}$$

Since

$$g(s) = \int g'(s)\,\mathrm{d}s = sg'(s) - \int sg''(s)\,\mathrm{d}s, \tag{A 15}$$

it follows that

$$\mathbb{A}_{1111} = \frac{3}{4}\int_0^{\infty}\frac{s\,\mathrm{d}s}{(b_1+s)^{5/2}\sqrt{b_2+s}\sqrt{b_3+s}}. \tag{A 16}$$

To show (2.10), again it is only necessary to prove this in the case when $\boldsymbol{B}$ is diagonal. The following identities are useful. If $\boldsymbol{U}$ and $\boldsymbol{V}$ are diagonal matrices, then

$$\left.\begin{aligned}\mathscr{S}(\boldsymbol{UV})_{iiii} &= U_{ii}V_{ii},\\ \mathscr{S}(\boldsymbol{UV})_{iijj} &= \tfrac{1}{6}(U_{ii}V_{jj}+U_{jj}V_{ii}), \quad \text{if } i\neq j\\ \mathscr{S}(\boldsymbol{UV})_{iijk} &= 0, \quad \text{if } i\neq j \text{ and } j\neq k,\end{aligned}\right\} \tag{A 17}$$

where no summation is implied for repeated indices.

Next, we show that the mapping from $\boldsymbol{B}$ to $\boldsymbol{A}$ defined by (2.7) is one-to-one and onto. This is equivalent to showing that the map from $\{(b_1,b_2,b_3) : b_1,b_2,b_3>0,\ b_1b_2b_3=1\}$ to $\{(\boldsymbol{A}_{11},\boldsymbol{A}_{22},\boldsymbol{A}_{33}) : \boldsymbol{A}_{11},\boldsymbol{A}_{22},\boldsymbol{A}_{33}>0,\ \boldsymbol{A}_{11}+\boldsymbol{A}_{22}+\boldsymbol{A}_{33}=1\}$ defined by (2.8) is one-to-one and onto. To this end, consider the map γ that takes (s,t) to the values of $(\boldsymbol{A}_{11},\boldsymbol{A}_{22})$ when $(b_1,b_2,b_3)=(\mathrm{e}^{s+t},\mathrm{e}^{s-t},\mathrm{e}^{-2s})$. In figure 2, we show how γ maps a grid in the s–t plane to the $\boldsymbol{A}_{11}$–$\boldsymbol{A}_{22}$ plane, providing a 'picture proof' that the map is one-to-one and onto.

To show that the map is one-to-one, it is sufficient to show that $\gamma(s,t)$ gives a family of curves with negative slope if s is fixed, and t is allowed to range freely, and that $\gamma(s,t)$ gives a family of curves with positive slope if the roles of s and t are reversed.

For example, let us prove that $\partial\boldsymbol{A}_{11}/\partial t<0$. We have that $\partial\boldsymbol{B}/\partial t=\boldsymbol{G}\cdot\boldsymbol{B}$ with

$$\boldsymbol{G} = \begin{bmatrix}1 & 0 & 0\\ 0 & -1 & 0\\ 0 & 0 & 0\end{bmatrix}, \tag{A 18}$$

https://doi.org/10.1017/jfm.2011.165 Published online by Cambridge University Press

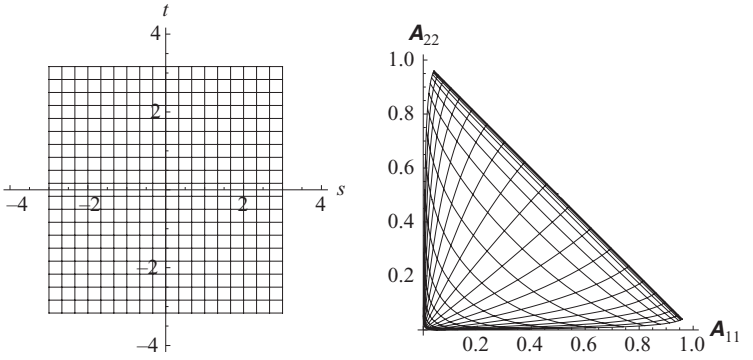


FIGURE 2. Diagram illustrating how γ maps a grid in the s–t plane to the $\boldsymbol{A}_{11}$–$\boldsymbol{A}_{22}$ plane.

that is $\boldsymbol{B}$ satisfies (2.4) with $\boldsymbol{E} = -\boldsymbol{G}$, $\boldsymbol{\Omega} = 0$, $\lambda = 1$ and $\boldsymbol{u} = 0$. (Since $\boldsymbol{B}$ is diagonal, we have $\boldsymbol{B}\cdot\boldsymbol{G} = \boldsymbol{G}\cdot\boldsymbol{B}$.) Hence, $\boldsymbol{A}$ satisfies (1.4) with the same parameters, and so $\partial \boldsymbol{A}_{11}/\partial t = -\boldsymbol{A}_{11} + \mathbb{A}_{1111} - \mathbb{A}_{1122} = -2\mathbb{A}_{1122} - \mathbb{A}_{1133} < 0$. Similarly, $\partial \boldsymbol{A}_{22}/\partial t > 0$, and hence $\gamma(s,t)$ gives a family of curves with negative slope if s is fixed and t is allowed to range freely.

To show that the map is onto, it is sufficient to see that the map γ 'stakes out' the appropriate region, which follows because $\gamma(s,t) \to (0,0)$ as $s \to \infty$, $\gamma(s,t)$ converges to a point on the line $\boldsymbol{A}_{11} + \boldsymbol{A}_{22} = 1$ as $s \to -\infty$, $\boldsymbol{A}_{11} \to 0$ as $t \to \infty$, and $\boldsymbol{A}_{22} \to 0$ as $t \to -\infty$.

For example, as $s \to -\infty$, we see from (2.2) that the fibre orientation distribution concentrates on the equator $p_3 = 0$. Hence, $\boldsymbol{A}_{33} \to 0$, and so $\boldsymbol{A}_{11} + \boldsymbol{A}_{22} = 1 - \boldsymbol{A}_{33} \to 1$. Since $\boldsymbol{A}_{11}$ and $\boldsymbol{A}_{22}$ increase as s decreases, they must also individually converge to limits.

REFERENCES

ADVANI, S. G. & TUCKER, C. L. 1987 The use of tensors to describe and predict fiber orientation in short fiber composites. *J. Rheol.* **31** (8), 751–784.

ALTAN, M. C., ADVANI, S. G., GÜÇERI, S. I. & PIPES, R. B. 1989 On the description of the orientation state for fiber suspensions in homogeneous flows. *J. Rheol.* **33** (7), 1129–1155.

ALTAN, M. C., SUBBIAH, S., GUCERI, S. I. & PIPES, R. B. 1990 Numerical prediction of three-dimensional fiber orientation in Hele-Shaw flows. *Polym. Engng Sci.* **30** (14), 848–859.

ALTAN, M. C. & TANG, L. 1993 Orientation tensors in simple flows of dilute suspensions of non-Brownian rigid ellipsoids, comparison of analytical and approximate solutions. *Rheol. Acta* **32**, 227–244.

BAY, R. S. 1991 Fiber orientation in injection molded composites: A comparison of theory and experiment. PhD thesis, University of Illinois at Urbana-Champaign.

BAY, R. S. & TUCKER, C. L. 1991 Fiber orientation in simple injection moldings. Part 1. Theory and numerical methods. In *Plastics and Plastic Composites: Material Properties, Part Performance, and Process Simulation* (ed. V. K. Stokes), *ASME*, vol. 29, pp. 445–471. American Society of Mechanical Engineers.

BIRD, R. B., ARMSTRONG, R. C. & HASSAGER, O. 1987 *Dynamics of Polymeric Liquids*, 2nd edn., vol. 1: *Fluid Mechanics*. Wiley.

BRETHERTON, F. P. 1962 The motion of rigid particles in a shear flow at low Reynolds number. *J. Fluid Mech.* **14**, 284–304.

CARLSON, B. C. 1995 Numerical computation of real or complex elliptic integrals. *Numer. Algorithms* **10**, 13–26.

CHUNG, D. H. & KWON, T. H. 2002 Invariant-based optimal fitting closure approximation for the numerical prediction of flow-induced fiber orientation. *J. Rheol.* **46** (1), 169–194.

https://doi.org/10.1017/jfm.2011.165 Published online by Cambridge University Press

Cintra, J. S. & Tucker, C. L. 1995 Orthotropic closure approximations for flow-induced fiber orientation. *J. Rheol.* **39** (6), 1095–1122.

Dinh, S. M. & Armstrong, R. C. 1984 A rheological equation of state for semiconcentrated fiber suspensions. *J. Rheol.* **28** (3), 207–227.

Doi, M. 1981 Molecular dynamics and rheological properties of concentrated solutions of rodlike polymers in isotropic and liquid crystalline phases. *J. Polym. Sci.* **19**, 229–243.

Folgar, F. P. & Tucker, C. L. 1984 Orientation behavior of fibers in concentrated suspensions. *J. Reinf. Plast. Compos.* **3**, 98–119.

GNU Scientific Library 2009 *GNU Scientific Library*. Available at: http://www.gnu.org/software/gsl.

Han, K.-H. & Im, Y.-T. 2002 Numerical simulation of three-dimensional fiber orientation in short-fiber-reinforced injection-molded parts. *J. Mater. Process. Technol.* **124**, 366–371.

Hinch, E. J. & Leal, L. G. 1976 Constitutive equations in a suspension mechanics. Part 2. Approximate forms for a suspension of rigid particles affected by Brownian rotations. *J. Fluid Mech.* **76**, 187–208.

Hobson, E. W. 1931 *Spherical and Ellipsoid Harmonic*. Cambridge University Press.

Jack D. A., Schache, B. K. & Smith, D. E. 2010 Neural network based closure for modeling short-fiber suspensions. *Polym. Compos.* **31** (7), 1125–1141.

Jack, D. A. & Smith, D. E. 2005 An invariant based fitted closure of the sixth-order orientation tensor for modeling short-fiber suspensions. *J. Rheol.* **49** (5), 1091–1116.

Jeffery, G. B. 1923 The motion of ellipsoidal particles immersed in a viscous fluid. *Proc. R. Soc. Lond. A* **102**, 161–179.

Lipscomb, G. G. II, Denn, M. M., Hur, D. U. & Boger, D. V. 1988 Flow of fiber suspensions in complex geometries. *J. Non-Newtonian Fluid Mech.* **26**, 297–325.

Montgomery-Smith, S. J., Jack, D. A. & Smith, D. E. 2010 A systematic approach to obtaining numerical solutions of Jefferys type equations using spherical harmonics. *Composites* A **41**, 827–835.

Montgomery-Smith, S. J., Jack, D. A. & Smith, D. E. 2011 The fast exact closure for Jeffery's equation with diffusion. *J. Non-Newtonian Fluid Mech.* **166**, 343–353.

Oberbeck, H. A. 1876 Über stationäre Flüssigkeitsbewegungen mit Berücksichtigung der inneren Reibeng. *Crelles J.* **81**, 62–87.

Press, W. H., Teukolsky, S. A., Vetterling, W. T. & Flannery, B. P. 2003 *Numerical Recipes in Fortran 77: The Art of Scientific Computing*, 2nd edn., vol. 1. Cambridge University Press.

Szeri, A. J. & Lin, D. J. 1996 A deformation tensor model of Brownian suspensions of orientable particles: the nonlinear dynamics of closure models. *J. Non-Newtonian Fluid Mech.* **64**, 43–69.

Verleye, V. & Dupret, F. 1993 Prediction of fiber orientation in complex injection molded parts. In *Developments in Non-Newtonian Flows* (ed. D. A. Signer), pp. 139–163.

VerWeyst, B. E. 1998 Numerical predictions of flow induced fiber orientation in three-dimensional geometries. PhD thesis, University of Illinois at Urbana Champaign.

VerWeyst, B. E. & Tucker C. L. III 2002 Fiber suspensions in complex geometries: Flow–orientation coupling. *Can. J. Chem. Engng* **80**, 1093–1106.

VerWeyst, B. E., Tucker, C. L., Foss, P. H. & O'Gara, J. F. 1999 Fiber orientation in 3-D injection molded features: Prediction and experiment. *Intl Polym. Process.* **14**, 409–420.

Wetzel, E. D. 1999 Modeling flow-induced microstructure of inhomogeneous liquid–liquid mixtures. PhD thesis, University of Illinois at Urbana Champaign.

https://doi.org/10.1017/jfm.2011.165 Published online by Cambridge University Press